

Unusual Exchange Bias in $\text{Sr}_2\text{FeIrO}_6/\text{La}_{0.67}\text{Sr}_{0.33}\text{MnO}_3$ Multilayer

K C Kharkwal, Rachna Chaurasia and A K Pramanik

School of Physical Sciences, Jawaharlal Nehru University, New Delhi - 110067, India

E-mail: akpramanik@mail.jnu.ac.in

Abstract. Here, we study an interface induced magnetic properties in $3d-5d$ based multilayer made of $\text{La}_{0.67}\text{Sr}_{0.33}\text{MnO}_3$ and double perovskite $\text{Sr}_2\text{FeIrO}_6$, respectively. Bulk $\text{La}_{0.67}\text{Sr}_{0.33}\text{MnO}_3$ is metallic and shows ferromagnetic (FM) ordering above room temperature. In contrast, bulk $\text{Sr}_2\text{FeIrO}_6$, is an antiferromagnet (AFM) with Néel temperature around 45 K (T_N) and exhibits an insulating behavior. Two set of multilayers have been grown on SrTiO_3 (100) crystal with varying thickness of FM layer. multilayer with equal thickness of $\text{La}_{0.67}\text{Sr}_{0.33}\text{MnO}_3$ and $\text{Sr}_2\text{FeIrO}_6$ (~ 10 nm) shows exchange bias (EB) effect both in conventionally field cooled (FC) as well as in zero field cooled (ZFC) magnetic hysteresis measurements which is rather unusual. The ZFC EB effect is weakened both with increasing maximum field during initial magnetization process at low temperature and with increasing temperature. Interestingly, multilayer with reduced thickness of $\text{La}_{0.67}\text{Sr}_{0.33}\text{MnO}_3$ (~ 5 nm) does not exhibit ZFC EB phenomenon, however, the FC EB effect is strengthened showing much higher value. We believe that an AFM type exchange coupling at interface and its evolution during initial application of magnetic field cause this unusual EB in present multilayers.

PACS numbers: 75.47.Lx, 75.70.Cn, 75.30.Et

1. Introduction

Artificially constructed interface between two dissimilar materials is of particular interest since new exotic states of matter emerge at interface which are not observed in its bulk counterpart. The interface properties in oxide materials have been widely studied during last several years showing many interesting physical properties which include unusual electronic transport and magnetism, superconductivity, ferroelectricity, exchange bias effect, etc.[1, 2, 3, 4, 5, 6, 7, 8, 9, 10, 11] Oxides, in general, has strong electronic correlation and complex interplay between charge, spin, orbital and lattice degrees of freedom. Therefore, confinement of electrons in nearly 2-dimensional (D) regime and reconstruction of charge, spin, orbital and lattice parameters at the interface are believed to cause such interesting properties. [12, 13, 14, 15, 16]

Among the oxide materials, while though $3d/4d$ based heterostructures have been extensively studied,[17, 18] the multilayers constituted with $3d/5d$ based materials are very less explored. The $3d/5d$ systems carry a special interest because in addition to conventional interfacial effect, these multilayers provide an ideal system to study an interplay between electron correlation (U) and spin-orbit coupling (SOC) effect.[19, 20] The $3d$ oxides usually show large U which is reduced in $5d$ materials due to its extended character of d orbitals. The $5d$ oxides, on the other hand, exhibit reasonable SOC with its heavy elements, therefore relevant energies share a comparable scale in these materials. Among $5d$ oxides, iridates have special interest. The high crystal field effect (CFE) splits d orbitals in these materials into t_{2g} and e_g states where a strong SOC further splits the low lying t_{2g} states into $J_{eff} = 3/2$ quartet and $J_{eff} = 1/2$ doublet.[21, 22] This gives a magnetic Ir^{4+} ($5d^5$) and non-magnetic Ir^{5+} ($5d^4$) with $J_{eff} = 1/2$ and 0 ground state, respectively. Hence, the electro-magnetic properties are largely tunable in iridates. Ir based oxides have recently been focused and therefore a detail investigation on both bulk as well as thin films are required to understand their properties.[23, 24, 25]

Here, we have studied an interface induced magnetic properties through exchange bias (EB) phenomenon in multilayers composed of $3d$ based $\text{La}_{0.67}\text{Sr}_{0.33}\text{MnO}_3$ (LSMO) and $3d$ - $5d$ based double perovskite (DP) $\text{Sr}_2\text{FeIrO}_6$ (SFIO) materials. The LSMO shows ferromagnetic (FM) ordering down to low temperature with transition temperature (T_c) above room temperature.[26] The $3d$ - $5d$ based DP systems are of recent interest because complex interaction between U and SOC can be studied in same DP materials. Our recent study shows bulk SFIO is insulating down to low temperature and exhibits prominent antiferromagnetic (AFM) ordering at temperature ~ 45 K (T_N), however, a weak AFM ordering has also been observed around 120 K. Magnetism in SFIO is only realized through Fe^{3+} ($3d^5$) channel as Ir^{5+} ($5d^4$) appears to be nonmagnetic within the picture of strong SOC.[27] The interface in present multilayer represent a meeting point of FM and AFM magnetic state with three different transition metals (Mn, Fe and Ir) which is rather uncommon.[41, 42, 24, 25] This FM/AFM based multilayer and interface is of further interest considering present developments in the field of AFM based spintronics and its applications.[28]

The EB effect manifest through shifting of magnetic hysteresis loop ($M(H)$) along the magnetic field axis when the system is cooled in magnetic field from above T_N , and an interface between FM and AFM state works a precursor. It is mostly believed that the process of field cooling induces an unidirectional FM anisotropy at the interface which causes EB effect. Apart from its fundamental interest, EB phenomenon has widely been studied with interest for technological applications such as, in magnetic storage, magnetic sensors, spintronics, etc.[29, 30, 31] Conventionally, $M(H)$ loop shifts to negative field direction when cooled in positive magnetic field or vice versa which is called as negative EB effect. There are, however, few reports which shows EB effect even when the system is cooled in zero magnetic field, which is known as zero field cooled (ZFC) EB or spontaneous EB effect.[32, 33, 34] Artificially designed multilayers are naturally the best choices for EB systems as not only an individual layer component can be chosen with particular magnetic state but the interface play crucial role here with a modified magnetic character. However, the technological challenges to observe the spin structure at the interface often impose difficulties to completely understand this EB phenomenon in multilayers.[35, 36, 37, 38, 39, 40]

In this present study, we have deposited epitaxial multilayers of [SFIO/LSMO]₃ with different layer thickness on SrTiO₃ (100) single crystal substrate and investigated the detailed magnetic properties. With lowering in temperature, magnetization continuously increases following pattern of LSMO, however, below around 45 K (T_N of SFIO) magnetization data show a large bifurcation between zero field cooled and field cooled process. Multilayer with equal layer thickness of LSMO and SFIO exhibit EB effect in both ZFC and FC $M(H)$ hysteresis loop, however, with decreasing thickness of FM LSMO the ZFC EB effect vanishes. The calculated EB field H_{EB} has been found to decrease with increase of applied field at 5 K in ZFC $M(H)$ data. Further, both the coercive field and the exchange bias both decreases with increasing temperature and the H_{EB} almost vanishes when temperature increases to T_N of SFIO.

2. Experimental details

Multilayers of Sr₂FeIrO₆ (SFIO) and La_{0.67}Sr_{0.33}MnO₃ (LSMO) have been deposited on SrTiO₃ (100) single crystal substrate using pulsed laser deposition (KrF, 248 nm) technique with laser energy density ~ 1.3 J/cm² and frequency 5 Hz. Substrate to target distance is kept around 5 cm and the deposition of both films has been done at 700°C to get good quality film. While deposition, oxygen pressure is maintained at ~ 0.1 mbar. After deposition the chamber is filled with oxygen at pressure around 500 mbar and then normally cooled to room temperature. The Polycrystalline target materials of SFIO and LSMO have been prepared by solid state method and characterized with x-ray diffraction (XRD). First, a layer of LSMO is deposited on SrTiO₃ and then SFIO is deposited. This has been repeated three times to get multilayer of the form [SFIO/LSMO]₃. Two sets of multilayer are deposited, namely SL_{10/10} and SL_{10/5} where the thickness of SFIO/LSMO has been kept as 10/10 and 10/5 nm, respectively. The growth rate for film deposition

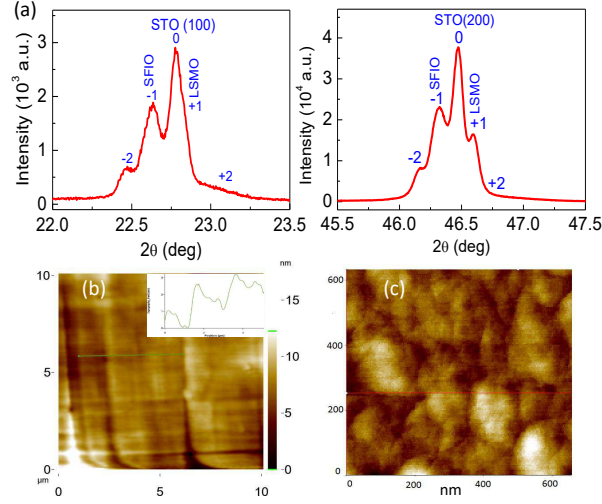


Figure 1. (color online) (a) shows x-ray diffraction pattern of $SL_{10/10}$ multilayer for (100) and (200) plane at left and right panel, respectively. (b) and (c) show the atomic force microscope (AFM) image of $SL_{10/10}$ multilayer with large area (unit micro-m) and small area (unit nano-m) scanning, respectively.

has been determined using a test film which is deposited using 8000 shots of laser with above mentioned parameters. A step has been introduced while deposition of film using a clip where the step height corresponds to the thickness of film. A field-emission scanning electron microscope (FESEM) has been used to measure the thickness of deposited film while a thickness profilometer and an atomic force microscope (M/s Nanomagetics) has been used to measure the depth of introduced step in film. Crystalline quality of the film has been checked with x-ray diffraction (XRD) measurements (PANalytical X'pert PRO) using $Cu K_\alpha$ x-ray source. Surface morphology of the film has been checked using atomic force microscope Magnetization measurements have been done using a vibrating sample magnetometer (PPMS by Quantum Design).

3. Result and discussion

Fig. 1a shows XRD pattern for $SL_{10/10}$ where the data at left and right panel represents (100) and (200) planes, respectively. The films are found to be epitaxial, adopting the structure of substrate. Figure shows both superlattice peaks and (weak) thickness fringes for both peaks, where the XRD peaks for SFIO and LSMO are observed at left and right side of STO, respectively (marked as -1 and $+1$). Lattice parameters of SFIO and LSMO, $SrTiO_3$ are calculated from the XRD pattern. The lattice parameters for SFIO, LSMO are 3.91 \AA , 3.88 \AA respectively, whereas 3.9 \AA for $SrTiO_3$. Similar, XRD pattern has been observed for $SL_{10/5}$, where peaks become less broaden (Not shown). Lattice mismatch between substrate and film has an interesting effect which induces strain and modifies the physical properties accordingly.[12] The lattice mismatch (Δa) has been calculated from XRD pattern using the formula

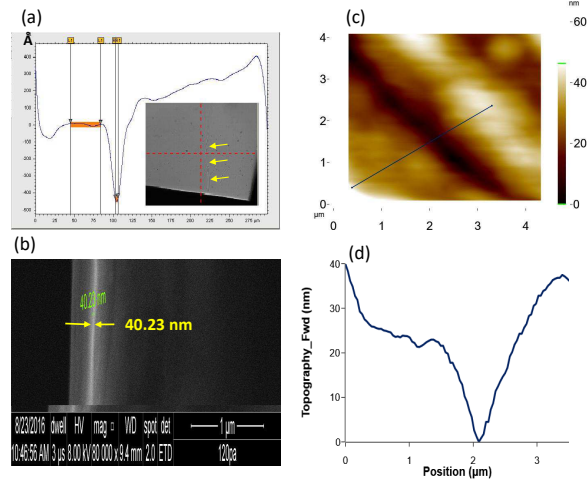


Figure 2. (color online) (a) shows depth profile of single layer thin film with film thickness around 40 nm. Inset shows surface of the film while horizontal arrows indicate the step in the film introduced during deposition of the film. (b) shows cross-sectional FESEM image same thin film showing film thickness ~ 40 nm. (c) shows AFM image of the same film collected across the step. (d) shows line profile of AFM image indicating depth of the step around 40 nm.

$$\Delta a(\%) = \frac{a_s - a_{th}}{a_s} \times 100 \quad (1)$$

where a_s and a_{th} are the corresponding lattice parameter of substrate and thin film. The bulk lattice parameters of SFIO are $a = 5.5515$, $b = 5.5785$, $c = 7.8435$ Å with triclinic crystal structure and LSMO are $a = 5.4820$, $b = 5.4820$, $c = 13.4490$ Å with rhombohedral crystal structure.[27] Here, the lattice mismatch between SrTiO₃ and first mono layer i.e LSMO is around 0.51% where the film is supposed to be grown along a - b plane with c -axis of the thin film contracted. However, with successive growth lattice mismatch at the interfaces of LSMO and SFIO is 0.77%, where due to lattice mismatch c -axis of the film has been elongated. The thickness of whole multilayer (D) has been calculated using the position of superlattice peaks with following formula,[43]

$$D = \frac{(m - n)\lambda}{2(\sin \theta_m - \sin \theta_n)} \quad (2)$$

where, λ is the wavelength of x-rays used for XRD measurements, θ_m and θ_n are the position of m and n order peak. The D for (100) and (200) planes has been calculated to be around 54.9 and 61.4 nm, respectively, where both these values of D are close to expected total thickness (60 nm) of the present multilayer.

Atomic force microscope images of the multilayer SL_{10/10} are shown in Fig. 1b and 1c with large and small scan area, respectively. Fig. 1b shows terrace type growth following the surface of STO substrate where inset indicates the terrace height is around

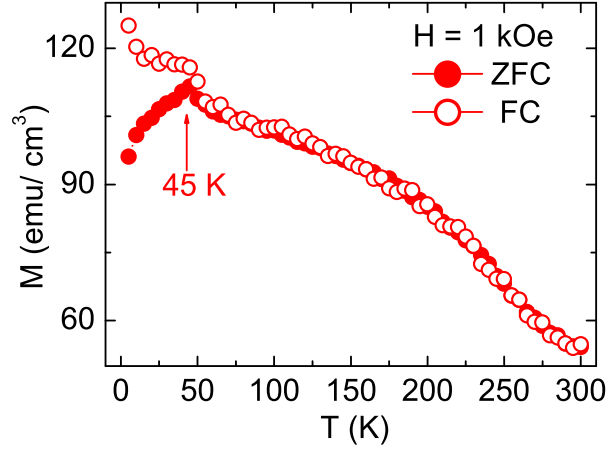


Figure 3. (color online) DC magnetization data measured in 1 kOe applied field under zero field cooled (ZFC) and field cooled (FC) protocol are shown as a function of temperature for $SL_{10/10}$ multilayer.

2 nm. The small area scanning in Fig. 1c shows growth pattern of present multilayer. The root mean square (rms) roughness of the film has been found to be about 1.8 nm, which is suggestive of good quality of film.

Fig. 2a shows the depth profile plot, collected with profilometer, on surface of test film (deposited with 8000 laser shots) across the introduced step which indicates step height is about 41 nm. A cross-sectional FESEM image of film has been shown in Fig. 2b indicating thickness of film around 40.2 nm. Fig. 2c presents an atomic force microscope image on film surface across the step. The line profile of microscope image has been shown in Fig. 2d which implies step height ~ 40 nm. The Fig. 2, as a whole, suggests the average thickness of film deposited with 8000 laser shots is around 40 nm which has been used for growth rate calibration.

Fig. 3 shows temperature dependent magnetization $M(T)$ data measured in 1000 Oe following zero field cooled (ZFC) and field cooled (FC) protocol for $SL_{10/10}$. With cooling, both M_{ZFC} and M_{FC} increases following the magnetic nature of LSMO which develops FM ordering at temperature above the room temperature. However, at low temperature around 45 K the M_{ZFC} exhibits a kink and below this temperature a wide bifurcation is observed between the ZFC and FC magnetization data. It can be noted that bulk Sr_2FeIrO_6 exhibits an AFM transition and onset of bifurcation between ZFC and FC $M(T)$ data around 45 K (T_N).[27] Similar AFM type magnetic transition at same temperature has been observed in Sr_2FeIrO_6 thin film (Fig. 3), although the nature of bifurcation in present multilayer is quite different than bulk Sr_2FeIrO_6 . This kink in M_{ZFC} and bifurcation is likely due to an interface effect. In particular, the decrease of moment in ZFC data below 45 K suggests an AFM type spin coupling at the interface. On the other hand, increase of moment below T_N in FC data is probably due to an increase of FM type interaction at interface which is favored while cooling the sample in magnetic field.

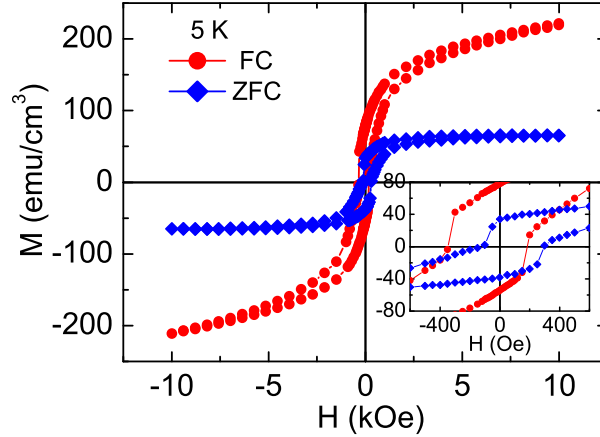


Figure 4. (color online) Field dependent magnetization data collected at 5 K following zero field cooled (ZFC) and field cooled (FC) protocol are shown for SL_{10/10} multilayer. Inset shows expanded view of the hysteresis loop near origin.

The field dependent magnetization data $M(H)$ collected following ZFC and FC protocol at 5 K with magnetic field range ± 10 kOe (H_{max}) are shown in Fig. 4 for SL_{10/10} multilayer. For ZFC data, the sample is cooled from room temperature to the target temperature in zero magnetic field and then $M(H)$ data have been collected. We have varied maximum applied field H_{max} in ZFC measurements at 5 K. For FC $M(H)$ data, the system has been cooled in presence of magnetic field (H_{cool}) to the target temperature and then field is swept from $+H_{cool}$ to $-H_{cool}$ and then to $+H_{cool}$. For both ZFC and FC $M(H)$ data, substrate (diamagnetic) contribution has been corrected using a slope in $M(H)$ data taken at high field regime of ZFC $M(H)$. The moment value in all $M(H)$ data represents contribution from both SFIO and LSMO layers. As evident in Fig. 4, magnetic moment in ZFC $M(H)$ initially increases steeply till $H \sim 1$ kOe and then the increase of $M(H)$ is rather slow. This initial fast increase of $M(H)$ is probably due to LSMO which is soft FM and shows saturation above ~ 1 kOe.[44] The SFIO is a hard AFM, therefore, ZFC $M(H)$ shows a slow increase or nearly saturation around 1 kOe field.[27] FC $M(H)$ data, on the other hand, continuously increase and it has much higher value compared to ZFC $M(H)$. This further indicates an AFM type spin interaction between LSMO and SFIO at interface. During FC process, the magnetic field couples with the interfacial spins while cooling through T_N of SFIO and induces FM like exchange which basically softens the spin alignment. Therefore, $M(H)$ shows a continuous increase in higher field regime.

Interestingly, both ZFC and FC $M(H)$ data show an asymmetry i.e., $M(H)$ loop is shifted (inset of Fig. 4). We observe H_c^L and $H_c^R = -346.1$ and 183.8 Oe, and M_r^U and $M_r^L = 78.3$ and -54.2 emu/cc, respectively. However, the direction of shifting is opposite in ZFC $M(H)$ data which moves to positive field and negative moment axis. We find $H_c^L = -127.4$ and $H_c^R = 296.4$ Oe, and $M_r^U = 34.0$ and $M_r^L = -38.3$ emu/cc. The H_c^L and H_c^R are the left and right coercive field, respectively where the moment becomes zero. Similarly, M_r^U and M_r^L are the upper and lower moment value, respectively at $H = 0$.

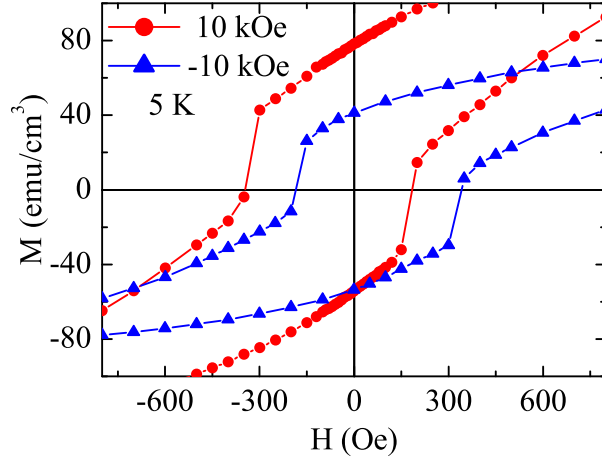


Figure 5. (color online) Field dependent magnetization data collected at 5 K following field cooled (FC) protocol with cooling field +10 kOe and - 10 kOe respectively are shown for $SL_{10/10}$ multilayer.

The nature of shift as well as closing of loops implies an EB effect in present multilayer. We have calculated the exchange bias field (H_{EB}) and effective coercive field H_c using $H_{EB} = (|H_c^L + H_c^R|)/2$ and $H_c = (|H_c^L - H_c^R|)/2$, respectively. For FC $M(H)$, we find $H_{EB} = 81.2$ and $H_c = 265$ Oe, respectively. Similarly, ZFC $M(H)$ data give $H_{EB} = 84.5$ and $H_c = 211.9$ Oe, respectively. It is though surprising that EB effect has been observed in both ZFC and FC $M(H)$ data in same system which is very uncommon. It can be noted that exchange bias has not been observed in single layer thin film of LSMO and SFIO deposited on $SrTiO_3$ substrate (Not shown). Conventionally, magnetic loop shifting occurs due to an unidirectional FM anisotropy when FM/AFM interface is cooled in magnetic field. The $M(H)$ loop generally shifts in opposite direction of cooling field i.e., shifts toward negative field when cooled in positive field which is called as negative EB effect.[29, 30, 31] It is further believed that FM type spin exchange coupling at FM/AFM interface renders an unusual EB effect. However, there are only few studies which have reported $M(H)$ loop shifting, normally toward positive field axis, even cooling in zero magnetic field which is known as positive or spontaneous EB effect. An AFM type spin interaction is argued for this positive EB effect which has been observed only in few systems.[32, 33, 34] Nonetheless, this ZFC EB effect is quite intriguing as the prerequisite unidirectional anisotropy, which is otherwise induced during FC process, can be realized isothermally in ZFC process.

To confirm the exchange bias effect in present multilayer, we have collected FM $M(H)$ data after cooling in both positive and negative applied field at 5 K. Fig. 5 shows $M(H)$ hysteresis loop close to the origin for cooling field of +10 and -10 kOe field. As evident in figure that for positive field cooling the $M(H)$ shifts to negative field axis and for negative field cooling the $M(H)$ shows opposite shifting. However, the shifting of $M(H)$ is almost equal. We calculate the $|H_{EB}|$ around 81 Oe in both cases. This confirms the exchange bias phenomena in present multilayer.

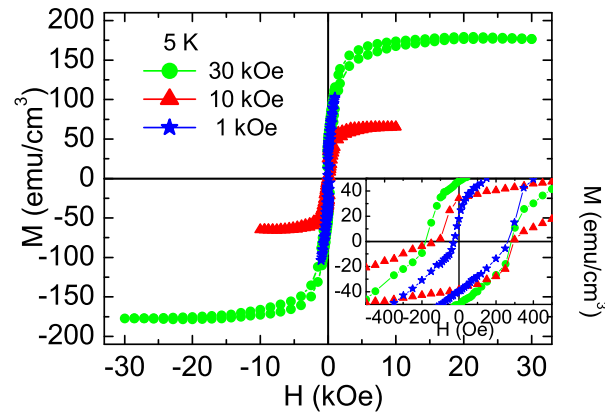


Figure 6. (color online) Field dependent magnetization data collected at 5 K following zero field cooled (ZFC) protocol are shown with maximum field 1 kOe, 10 kOe and 30 kOe respectively, for $SL_{10/10}$ multilayer. Inset shows expanded view of the hysteresis loop near origin.

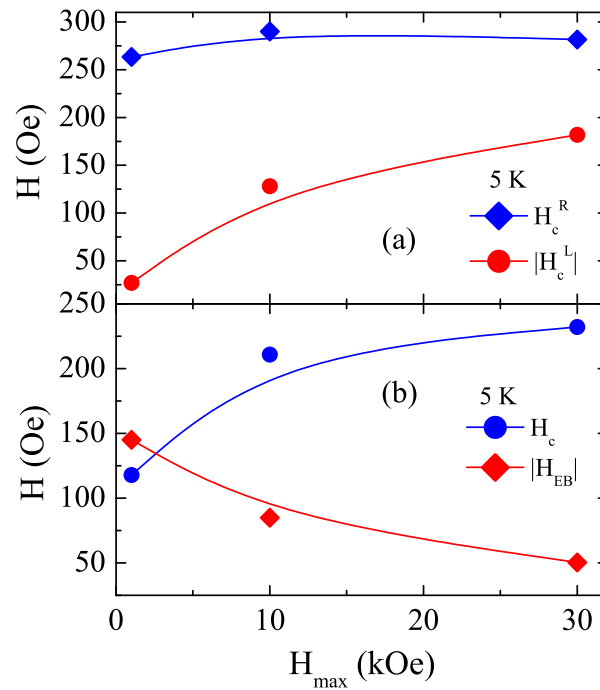


Figure 7. (color online) (a) Right (H_c^R) and left (H_c^L) coercive fields are shown as a function of maximum applied field (H_{max}) that are obtained in ZFC $M(H)$ measurements for $SL_{10/10}$ multilayer at 5 K. (b) shows calculated coercive (H_c) and exchange bias ($|H_{EB}|$) field as a function of maximum field at 5 K (see text).

In order to understand the ZFC EB effect in further detail, we have measured $M(H)$ loops at 5 K with different maximum applied field H_{max} for SL_{10/10}. Fig. 6 shows $M(H)$ plots with $H_{max} = 1, 10,$ and 30 kOe at 5 K. As evident in figure, while $M(H)$ data for $H_{max} = 10$ and 30 kOe show almost saturation, the data for $H_{max} = 1$ kOe show no sign of saturation. Inset of Fig. 6 shows expanded view of same plot near the origin. It is surprising that the moment in ZFC $M(H)$ increases substantially with applied field, H_{max} . Out of Mn, Fe and Ir transition metals, only Mn (mixture of Mn⁺³ and Mn⁺⁴) and Fe⁺³ contribute to moment as Ir⁺⁵ is supposed to be nonmagnetic.[27] This implies the saturation moment for LSMO and SFIO would be 3.7 and $5 \mu_B/\text{f.u.}$, respectively. We, however, experimentally find moment around 0.807 and $2.193 \mu_B/\text{f.u.}$ in ZFC $M(H)$ for 10 and 30 kOe field (Fig. 6), respectively considering only LSMO layers. This indicates even FM LSMO layer is not fully saturated which is probably due to surface/interface disorder and finite-size effect in films. It has been previously shown that both the transition temperature T_c as well as moment is significantly modified with layer thickness in LSMO film.[45, 46, 47] The Figure 6 suggests that initially with increasing field the moment in LSMO layers and at interfaces increases which gives different values of moment at different fields. However, the moment in AFM type SFIO layer does not increase much, and as a resultant it gives almost saturated value in higher field regimes.

All the $M(H)$ plots show shifting toward positive field axis i.e., ZFC EB effect, however, nature of shifting changes with H_{max} . For $H_{max} = 1$ kOe, we find H_c^L and H_c^R values are around 27 and 263 Oe, and M_r^U and M_r^D values are about 17.8 and 39.3 emu/cc, respectively. While though $M(H)$ does not saturate with $H_{max} = 1$ kOe but the H_c^L closely matches with that for LSMO films.[26, 44, 45, 46, 47] The high value of H_c^R probably arises due to locking of spin at the interface of LSMO/SFIO which causes positive EB effect. With increasing H_{max} , Fig. 7 shows while H_c^R does not change appreciably but H_c^L increases significantly and tends to approach H_c^R . In Fig. 7a, we have shown the variation of both H_c^R and H_c^L with H_{max} at 5 K for SL_{10/10} multilayer. The calculated H_{EB} and H_c are shown in Fig. 7b which shows H_{EB} decreases and H_c increases with H_{max} .

We have further checked the effect of temperature on EB effect. We have measured ZFC $M(H)$ loop with $H_{max} = 10$ kOe at different temperatures for SL_{10/10} multilayer. The calculated H_{EB} and H_c are presented in Fig. 8 showing both the values decrease monotonically with temperature. The H_{EB} almost vanishes (~ 4 Oe) once temperature is raised to 30 K which is close to T_N (~ 45 K) of AFM component SFIO. With increasing temperature, the AFM anisotropy in SFIO weakens which consequently reduces the EB effect.

In Fig. 9, we propose a schematic model for spin alignment with magnetic field of SL_{10/10} multilayer during ZFC $M(H)$ process. It is clear in Fig. 6 that the externally applied H_{max} has significant influence on the the spin interaction in present multilayer system. For example, asymmetric behavior in $M(H)$ is reduced where the H_c^L increases which gives a decreasing exchange bias effect with increasing H_{max} (see Fig. 7). Given

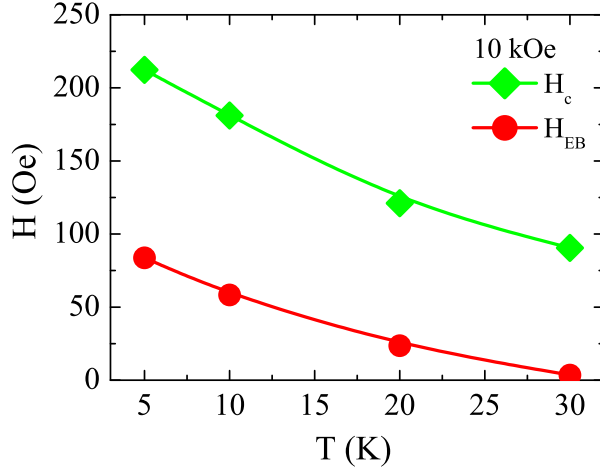


Figure 8. (color online) Variation of coercive and exchange bias field is shown with temperature in zero field cooled (ZFC) field dependent magnetization for $SL_{10/10}$ multilayer.

that two magnetic component in present multilayer are FM (LSMO) and AFM (SFIO) and it shows different EB in ZFC, therefore an AFM type interface exchange interaction expected. In Fig. 9, we have focused on a representative tri-layer of LSMO/SFIO/LSMO (FM/AFM/FM) showing two interfaces. While there are many domains of different spin orientation in each layer, for simplicity, we have considered only two domains (Region I and II) in each layer with different crystal easy axis in parallel and anti-parallel to applied field. It can be further noted that there are very limited reports of neutron diffraction measurements at low temperature magnetic state (5 K) for SFIO to understand the AFM spin structure or the nature of magnetic exchange interaction.[48, 49] The study shows a nearest neighbor type exchange interaction among magnetic Fe^{+3} ions but the nature of AFM type has not been discussed. In Fig. 9, we have assumed a simple AFM spin structure where an alternative layer has opposite orientation which is close to A-type AFM. This has been shown to schematically demonstrate the interface exchange interaction. Nonetheless, experimental efforts are required to understand the AFM spin structure in SFIO.

Fig. 9a shows the tri-layer assembly with an AFM type interface at 5 K under ZFC condition. When the applied magnetic field during first application of magnetic field in $M(H)$ measurement is low and below the threshold value H_{Th} , the LSMO spins (Region II) will align to the direction of magnetic field due to its low anisotropy (Fig. 9b). The antiferromagnetically ordered spins in hard SFIO will, however, not be influenced at low magnetic field. This LSMO spin alignment will reconstruct the AFM-type interface in Region II (Fig. 9b). With further increase in magnetic field above H_{Th} , the SFIO spins in the vicinity of interface will align to the direction of magnetic field because at interface generally has low anisotropy compared to bulk of material. This spin alignment conversion will advance the interface toward inside of AFM SFIO layer which would effectively increase the thickness of FM layer. More the applied field, less would be the

separation between FM layer as shown at Fig. 9c. When the applied magnetic field H_{max} is sufficiently high, an effective thickness of AFM layer will reduce substantially which will facilitate an indirect or tunneling exchange interaction between the adjacent FM layers due to their inter-layer separation.[32] This tunneling exchange is induced by applied magnetic field and would help to retain the moment even field decreases to zero. This tunneling exchange is similar to exchange interaction as observed in cases of cluster glass or super-ferromagnetic interaction.[50] While the AFM spin ordering in SFIO will be the least influenced by field sweeping but there tunneling exchange among the FM layers will obstruct the rotation of FM spin in LSMO with field, which will result in an increased M_r^U and H_c^L .

The effect of tunneling FM exchange is evident in Fig. 6 as with increasing H_{max} , both the remnant moment M_r^U as well as the coercive field H_c^L increases. The decreasing exchange bias effect (H_{EB}) with increasing H_{max} (Fig. 7) can be explained with an indirect FM coupling among the FM layers in present multilayer system. In present model, we have considered only FM/AFM domains with anisotropy axis parallel and/or anti-parallel to the applied magnetic field for simplicity. However, domains with easy axis making finite angle with magnetic field will also result in exchange bias effect.[32] Here, it can be mentioned that tuning of ZFC exchange bias effect through applied magnetic field has been previously observed in Ni-Mn-In bulk alloys where the superparamagnetic domains embedded in AFM host are shown to grow with the field which engage in tunneling exchange interaction that modifies both the coercive fields and consequently exchange bias effect.[32] The remnant magnetization M_r^U as well as H_c^L increase with H_{max} which implies a new complex magnetic state has been established in this multilayer which has altered the EB effect. The significant aspect of present SL_{10/10} multilayer is that it exhibits EB effect with reasonable H_{EB} in a simplified ZFC condition. Moreover, it requires low magnetic field which is in contrast with other reported studies where higher magnetic fields have been applied.[32, 33] Nonetheless, tuning of exchange bias effect in present heterostructure system with magnetic field is quite noteworthy.

To further understand the role of individual FM and AFM layer on EB effect, we have prepared another [SFIO/LSMO]₃ multilayer SL_{10/5} keeping layer thickness of SFIO and LSMO around 10 and 5 nm, respectively. Fig. 10 shows both ZFC and FC $M(H)$ plots of SL_{10/5} at 5 K. Unlike the SL_{10/10} multilayer, ZFC $M(H)$ data of SL_{10/5} surprisingly do not show any sign of saturation at high magnetic field, rather it increases continuously till measuring field of 10 kOe and shows higher value than FC $M(H)$ (Figs. 4 and 10). The expanded view of $M(H)$ data close to the origin has been shown in inset of Fig. 10. With stark contrast, ZFC $M(H)$ of SL_{10/5} does not exhibit any appreciable asymmetry in terms of magnetic field of magnetization i.e., it does not show EB effect. However, reasonable negative shifting of $M(H)$ data is observed for FC $M(H)$. We find $H_c^L = -1048.5$ and $H_c^R = 617.0$, and $M_r^U = 61.1$ and $M_r^D = -44.2$ emu/cc which gives $H_{EB} = 215.7$ and $H_c = 832.7$ Oe. These (FC) values of both H_{EB} and H_c are much higher compared to previously discussed SL_{10/10} multilayer at same temperature

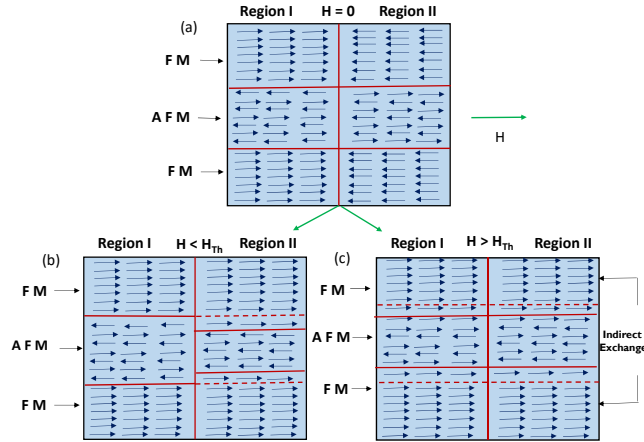


Figure 9. (color online) Schematic diagram representing the spin interaction during ZFC $M(H)$ measurement is shown at 5 K for $SL_{10/10}$ multilayer. (a) shows spin arrangement at $H = 0$ before application of magnetic field while (b) and (c) show the same at $H < H_{Th}$ and $H > H_{Th}$, respectively (see text). Vertical lines separate two region with opposite anisotropy axis, the bold horizontal lines represent FM/AFM interface while broken horizontal lines represent the position of original interface in this multilayer.

and with same H_{max} . The effect of FM layer thickness on EB effect has been discussed theoretically which predicts $H_{EB} \propto 1/t_{FM}$, where t_{FM} is FM layer thickness.[30, 37] With decreasing t_{FM} , the FM spins are more firmly locked with AFM layer through interface exchange coupling therefore, FC spin rotation shows higher H_c^L during field sweeping in $M(H)$. In that sense, the increase of both H_{EB} and H_c in $SL_{10/5}$ multilayer is quite explained through decrease of FM layer thickness. Disappearance of EB effect in ZFC $M(H)$ with decreasing FM layer thickness in $SL_{10/5}$ is quite intriguing. The ZFC $M(H)$ for $SL_{10/5}$ shows $H_c^L \sim H_c^R \sim 430$ Oe which are higher than the respective values for $SL_{10/10}$. Though there would be an expansion of FM layer thickness during application of initial magnetic field in ZFC $M(H)$ but the t_{FM} will still be thin enough where the FM spins are firmly locked with adjacent AFM spins through interface. This would render a symmetric ZFC $M(H)$ without EB effect. Nonetheless, presence of both ZFC and FC EB effect in same system with reasonable bias field H_{EB} in low magnetic field is quite noteworthy and requires further investigation using both theoretical and microscopic experimental tools.

4. Conclusions

Epitaxial multilayers of $3d-5d$ based $La_{0.67}Sr_{0.33}MnO_3$ and double perovskite Sr_2FeIrO_6 have been deposited on single crystal $SrTiO_3$ (100) using pulsed laser deposition technique. The magnetic states of bulk $La_{0.67}Sr_{0.33}MnO_3$ and Sr_2FeIrO_6 are respectively ferromagnetic with T_c above room temperature and AFM with ordering temperature $T_N \sim 45$ K. An onset of antiferromagnetic type magnetic exchange coupling at interface

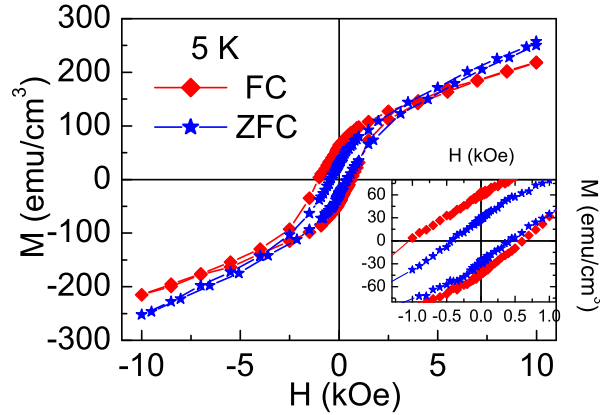


Figure 10. (color online) Zero field cooled (ZFC) and field cooled (FC) magnetization data are shown as a function of magnetic field collected at 5 K for $SL_{10/5}$ multilayer. Inset shows expanded view of the hysteresis loop near origin.

is evident in temperature dependent magnetization data below T_N of Sr_2FeIrO_6 . Interestingly, multilayer with ~ 10 nm of individual layer thickness exhibits both FC and ZFC exchange bias effect. While the EB effect after FC is conventional but the positive EB effect after ZFC is quite unusual and rarely observed. In ZFC $M(H)$, it is believed that FM layer thickness increases with field and a tunneling exchange coupling is established among the FM layers which basically weakens the ZFC EB effect with increasing maximum applied field. Similarly, ZFC EB effect decreases with increasing temperature which is due to weakening of AFM anisotropy. The $3d-5d$ interface is quite interesting due to presence of different competing energy scale. Therefore, more similar studies involving different transition metals are necessary to comprehend this complex behavior.

Acknowledgments

We acknowledge SERB, DST for supporting Excimer pulse laser and UPE-II, UGC for deposition chamber. We are also thankful to DST-FIST for supporting atomic force microscope, DST-PURSE for funding and IIT Delhi for magnetization measurements. KCK and RC acknowledge UGC, India for financial support.

References

- [1] Bert J A, Kalisky B, Bell C, Kim M, Hikita Y, Hwang H Y, and Moler K A, *Nature Physics* **7**, 2079, (2011).
- [2] Li L, Ritcher C, Mannhart J, and Ashoori R C, *Nature Physics* **7**, 2080, (2011).
- [3] Gibert M, Zubko P, Scherwitzl R, Iniguez J, and Triscone J M, *Nature Materials* **11**, 3224, (2012).
- [4] Grutter A J, Yang H, Kirby B J, Fitzsimmons M R, Aguiar J A, Browning N D, Jenkins C A, Arenholz E, Mehta V V, Alaan U S, and Suzuki Y, *Phys. Rev. Lett.* **111**, 087202, (2013).
- [5] Sanchez J C R, Cheeseman B N, Granada M, Aronholz E, and Steren L B, *Phys. Rev. B* **85**, 094427, (2012).

- [6] Nakamura Y and Yanase Y, *J. Phys. Soc. Jpn.* **82**, 083705, (2013).
- [7] Ganguli N and Kelly P J, *Phys. Rev. Lett.* **113**, 127201, (2014).
- [8] Reyren N, Thiel S, Caviglia A D, Kourkoutis L F, Hammerl G, Richter C, Schneider C W, Kopp T, Ruetschi A S, Jaccard D, Gabay M, Muller D A, Triscone J M, and Mannhart J, *Science* **317**, 1196, (2007).
- [9] Banerjee S, Erten O and Randeria M, *Nature Physics* **9**, 2702, (2013).
- [10] Dong S and Dagotto E, *Phys. Rev. B* **87**, 195116, (2013).
- [11] Ohtomo A and Hwang H Y, *Nature* **427**, 423, (2004).
- [12] Hwang H Y, Iwasa Y, Kawasaki M, Keimer B, Nagaosa N, and Tokura Y, *Nature Materials* **11**, 3223, (2012).
- [13] Chakhalian J, Freeland J W, Millis A J, Panagopolous C, and Rondinelli J M, *Rev. Mod. Phys.* **86**, 1189, (2014).
- [14] Zubko P, Gariglio S, Gabay M, Ghosez P, and Triscone J M, *Annu. Rev. Condens. Matter Phys.* **2**, 141, (2011).
- [15] Mannhart J and Schlom D G, *Science* **327**, 1607, (2010).
- [16] Hammerl G and Spaldin N, *Science* **332**, 922, (2011).
- [17] He C, Grutter A J, Gu M, Browning N D, Takamura Y, Kirby B J, Borchers J A, Kim J W, Fitzsimmons M R, Zhai X, Mehta V V, Wong F W, and Suzuki Y, *Phys. Rev. Lett.* **109**, 197202, (2012).
- [18] Padhan P and Prellier W, *Eur. Phys. J. B* **45**, 169, (2005).
- [19] Pesin D and Balents L, *Nat. Phys.* **6**, 376, (2010).
- [20] Samanta K and Dasgupta T Saha, *Phys. Rev. B* **95**, 235102, (2017).
- [21] Kim B J, Jin H, Moon S J, Kim J Y, Park B G, Leem C S, Yu J, Noh T W, Kim C, Oh S J, Park J H, Durairaj V, Cao G, and Rotenberg E, *Phys. Rev.Lett.* **101**, 076402 (2008).
- [22] Kim B J, Ohsumi H, Komesu T, Sakai S, Morita T, Takagi H, Arima T, *Science* **323**, 1329 (2009).
- [23] Nichols J, Gao X, Lee S, Meyer T L, Freeland J W, Lauter V, Yi D, Liu J, Haskel D, Petrier J R, Guo E J, Herklotz A, Lee D, Ward T Z, Eres G, Fitzsimmons M R, and Lee H N, *Nat. Comm.* **7**, 12721, (2016).
- [24] Yi D, Flint C L, Balakrishnan P P, Mahalingam K, Urwin B, Vailionis A, Diaye A T N, Shafer P, Arenholz E, Choi Y, Stone K H, Chu J H, Howe B, Liu J, Fisher, and Suzuki Y, *Phys. Rev. Lett.* **119**, 077201, (2017).
- [25] Okamoto S, Nichols J, Sohn C, Kim S Y, Noh T Y and Lee H N, *Nano Lett.* **17**, 2126, (2017).
- [26] Ettayfi A, Moubah R, Boutahar A, Hlil E K , Lassri H, *J. Supercond. Nov. Magn.* **29**, 133, (2016).
- [27] Kharkwal K C and Pramanik A K, *J. Phys.: Condens. Matter* **29** , 495801, (2017).
- [28] Baltz V, Manchon A, Tsoi M, Moriyama T, Ono T, and Tserkovnyak Y, *Rev. Mod. Phys.* **90**, 015005 (2016).
- [29] Gokemeijer N J and Chien C L, *J. Appl. Phys.* **85**, 5516, (1999).
- [30] Nogues J and Schuller I K, *J. Magn. Magn. Mater.* **192**, 203, (1999).
- [31] Nogues J et al., *Phys. Rep.* **422**, 65, (2005).
- [32] Wang B M, Liu Y, Ren P, Xia B, Ruan K B, Yi J B, Ding J, Li X G, and Wang L, *Phys. Rev. Lett.* **106**, 77203, (2011).
- [33] Saha J and Victora R H, *Phys. Rev. B* **76**, 100405, (2007).
- [34] Murthy J K and Venimadhav A K, *Appl. Phys. Lett.* **103**, 252410, (2013).
- [35] Meiklejohn W H and Bean C P, *Phys. Rev.* **102**, 1413, (1956).
- [36] Stamps R L, *J. Phys. D* **33**, R247, (2000).
- [37] Kiwi M, *J. Magn. Magn. Mater.* **234**, 584, (2001).
- [38] Berkowitz A E and Takano K, *J. Magn. Magn. Mater.* **200**, 552, (1999).
- [39] Ohldag H, Scholl A, Nolting F, Arenholz E, Maat S, Young A T, Carey M, and Stohr J, *Phys. Rev. Lett.* **91**, 017203, (2003).
- [40] Wu J, Park J S, Kim W, Arenholz E, Liberati M, Scholl A, Wu Y Z, Hwang C, and Qiu Z Q, *Phys. Rev. Lett.* **104**, 217204, (2010).

- [41] Fan M, Zhang W, Jian J, Huang J, and Wang H, *Appl. Phys. Lett. Materials* **4**, 076105, (2016).
- [42] Jia Y, Chopdekar R V, Arenholz E, Young A T, Marcus M A, Mehta A and Takamura Y, *Phys. Rev. B* **92**, 094407, (2015).
- [43] Kim K W, Ghosh S, Buvaev S, Hebard A F, and Norton D P, *J. Appl. Phys.* **119**, 215303, (2016).
- [44] Feng Y, Jin K J, Gu L, He X, Ge C, Zhang Q H, He M, Guo Q L, Wan Q, He M, Lu H B, and Yang G, *Scientific Reports* **6**, 22382, (2016).
- [45] Kourkoutis L F, Song J H, Hwang H Y, and Muller D A, *Proc. Natl. Acad. Sci. U.S.A.* **107**, 11682, (2010).
- [46] Huijben M, Martin L W, Chu Y H, Holcomb M B, Yu P, Rijnders G, Blank D H A, and Ramesh R, *Phys. Rev. B* **78**, 094413, (2008).
- [47] Chopdekar R V, Arenholz E, and Suzuki Y, *Phys. Rev. B* **79**, 104417, (2009).
- [48] BattlePD, BlakeGR, GibbTC and VenteJF, *J. Solid State Chem.* **145**,541 (1999).
- [49] QasimI, BlanchardPER, LiuS, TangC, KennedyBJ, AvdeevM and KimptonJA, *J. Solid State Chem.* **206**242 (2013).
- [50] Bedanta S and Kleemann W, *J. Phys. D* **42**, 013001 (2009).